

# Chapter 2

## Modelling Strategies and Two-Phase Flow Models

Geoffrey F. Hewitt and George Yadigaroglu

### 2.1 Two-Phase Flows and Their Analysis

We will recall first the general methods of solution of thermal-hydraulic problems and then show how these are complicated by the presence of multiphase flows before entering in the following sections into the descriptions of the various approaches.

#### 2.1.1 General Methods of Solution

The design and transient behaviour problems are treated in a similar manner. Starting from the general conservation laws:

- conservation of mass
- conservation of momentum
- conservation of energy,

we express these by *partial differential equations*. We choose the minimum required number of space variables and consider, if necessary, time dependence. Very often we deal with *one-dimensional systems* and with cross-sectionally averaged variables. We then “close” or complete the set of equations by including the necessary *constitutive laws and relations*, namely,

---

G.F. Hewitt (✉)

Department of Chemical Engineering and Chemical Technology,  
Imperial College, London, UK  
e-mail: g.hewitt@imperial.ac.uk

G. Yadigaroglu

ETH Zurich, Zurich, Switzerland  
e-mail: yadi@ethz.ch

- *equations of state* that govern the physical properties of the materials involved
- *general laws of nature or rate equations*, e.g. the Fourier law of conduction, Newton's law of viscosity, etc. These describe in an idealized or simplified manner natural behaviour. For multiphase flows, new needs appear in this category, or the corresponding laws become much more complex (e.g. how is heat conducted in a two-phase mixture)
- *semi-empirical* relations for parameters such as friction factors, heat transfer coefficients, turbulence parameters, etc. These often appear in the conservation equations because of the idealizations or reductions in space variables made, e.g. instead of resolving all details of the flow in three dimensions and getting the heat transfer law at the wall, we work in one dimension and use a heat transfer coefficient for the heat transfer between the wall and the average temperature of the fluid. Again, here the situation becomes much more complex for multiphase flows, e.g. in the determination of frictional pressure drop or of the heat transfer law in boiling. In particular, in two-phase flows, we should make sure that the empirical relations used remain valid in the domain of application as most available data cover rather narrow domains.

We then define the boundary conditions of the problem. These are prescribed according to our physical understanding of the problem and are often approximations of reality.

Finally, we solve the resulting set of equations subject to the boundary conditions. Exact analytical solutions are rare; approximate analytical solutions are sometimes possible; numerical methods embedded in computer codes are most often used.

As said in Chap. 1, we are dealing here mainly with one-dimensional systems and corresponding formulations. Multidimensional formulations of multiphase flow problems will be only briefly discussed below and treated in other volumes with methods based on Computational Fluid Dynamics (CFD).

### 2.1.2 *Special Features of Two-Phase Flows*

The most important feature of gas–liquid flows, when compared to single-phase flows, is the existence of deformable interfaces. This, coupled with the naturally occurring turbulence in gas–liquid flows, makes them highly complex. Some simplification is possible by classifying the types of interfacial distributions (their topology) under various headings, known as *flow regimes* or *flow patterns*. The two-phase flow regimes for gas–liquid flow in vertical tubes are illustrated in Fig. 2.1 and range from bubble flow to wispy annular flow. Vertical flows are, on average, axi-symmetric but with horizontal flows, gravity induces the liquid to move preferentially towards the bottom of the channel as shown in Fig. 2.2. Flow patterns and their prediction will be discussed in another chapter.

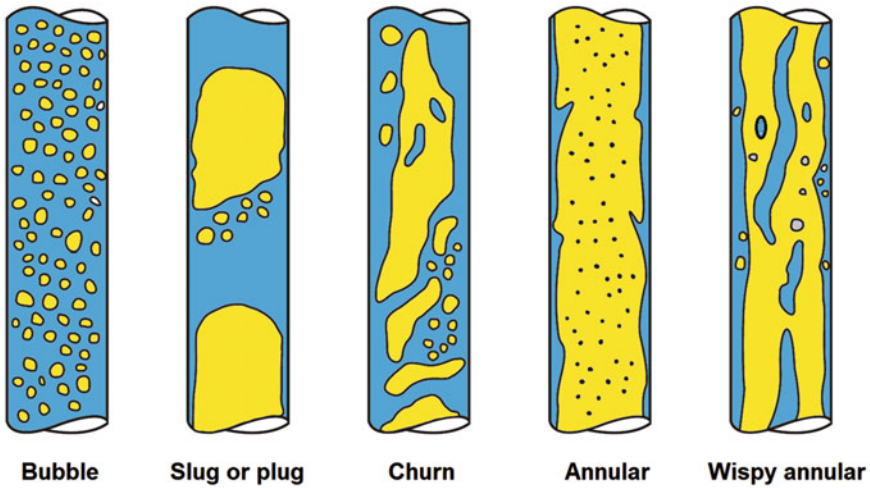


**Fig. 2.1** Main flow regimes in upwards gas-liquid flow in vertical tubes

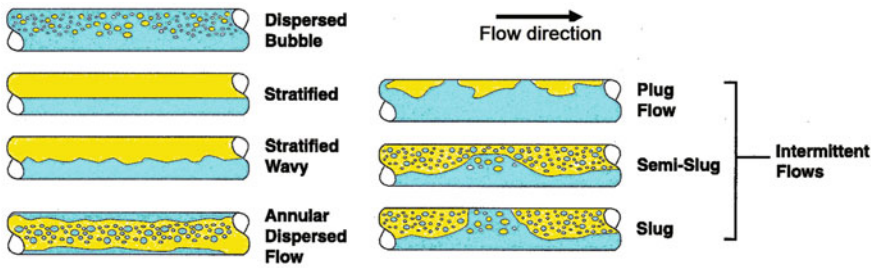


**Fig. 2.2** Main flow regimes in gas-liquid flow in horizontal tubes

An exact formulation of the two-phase flow problem would have required the description of the evolution in time of the fields (pressure, velocity, temperature, etc.) for each phase, together with a prediction of the geometry of the interfaces. Such an approach is impractical, except in some relatively very simple situations, for example in horizontal stratified flow, where the geometrical configuration of the two phases is a priori known or can be computed by interface tracking methods (discussed later in Sect. 2.7). In most situations, however, the flow field and the topographical distribution of the phases are chaotic and must be described using statistical, average properties. There are two general approaches, the *two-fluid approach* and the *mixture formulation*; we will discuss them in Sect. 2.5.

### 2.1.3 Two-Phase Flow Equipment

Two-phase gas–liquid flow is important in a wide variety of equipment types which include the following.

#### Vapour Generation Systems

In these systems, vapour is generated by the addition of heat and joins the liquid in flowing through the system. Vapour generation equipment includes power station boilers, waste heat boilers, coiled tube boilers and package boilers. Vapour generation is also a vital component of many process plants, with equipment ranging from fired heaters to various kinds of reboilers (kettle, horizontal thermosiphon and vertical thermosiphon). The generic problems in all this equipment are the prediction of void fraction and pressure drop (and hence pumping power or, in the case of natural circulation systems, circulation rate), critical heat flux, heat transfer, system stability and fouling of the heat transfer surfaces.

#### Nuclear Power Plants (NPP)

Vapour generation is also, of course, vital in nuclear power generation and can occur directly within the reactor itself (as in the Boiling Water Reactor, BWR) or in the steam generators which are heated by hot fluid from the reactor (as in the Pressurized Water Reactor, PWR). Two-phase flow and heat transfer with phase change are important for the normal operation of NPPs but become very complex in case of transient and accidental situations. A very large number of situations and phenomena can be encountered; these will be discussed in another volume in this series.

#### Vapour Condensers

Most condensers are of the *indirect contact* type and there is a preponderance of the shell-and-tube type of condenser, with both condensation on the tube side and the shell side. However, air-cooled condensers are important as are matrix (brazed aluminium) condensers for cryogenic systems, for instance. Condensation can also be carried out in the *direct contact* mode with various types of equipment being used (pool type condensers, spray condensers, baffle column condensers, etc.). Again, the principal requirements for design are prediction of void fraction and pressure drop and heat transfer coefficients. In many systems, the fluids are multi-component in nature and condensation involves simultaneous heat and mass transfer. Where the condensation is done in counter-current flow, flooding can be an important limitation on operation.

#### Mass Transfer Equipment

Many mass transfer operations (absorption, stripping, humidification, dehumidification, distillation, etc.) involve gas–liquid two-phase flows. Equipment used includes bubble columns, wetted wall columns, plate columns (having bubble caps or sieve plates, etc.), packed columns and spray chambers. Again, the key problems in design are the prediction of mass transfer coefficients and pressure

drop. However, questions of stability, bypass and phase separation are of considerable importance in this type of equipment.

In carrying out designs, information is required on the *fluid physical properties* and on the expected *flow rates* of the respective phases. The prediction requirements for design are of three categories:

- (1) *Steady-state design parameters*. These include pressure drop, heat and mass transfer laws and coefficients and mean gas phase content (void fraction).
- (2) *Limiting conditions*. These include critical heat flux (i.e. the heat flux at which the heat transfer coefficient deteriorates, possibly leading to damage of the channel surface), critical mass flux (the condition at which the flow rate becomes independent of downstream pressure), mechanical vibration, erosion and corrosion and instability.
- (3) *Plant transients*. These cover a whole range of situations including plant start-up and shutdown, emergency events (such as the loss of site power in a nuclear power station), Loss Of Coolant Accidents (LOCAs) and atmospheric release and dispersion of multiphase mixtures.

To meet the above design requirements, a number of approaches to prediction can be taken. These include

- (1) The empirical approach
- (2) Phenomenological modelling
- (3) Multi-fluid modelling
- (4) Computational fluid dynamics modelling (CFD).

These various approaches will be discussed in the following sections; each approach has limitations and there is no general “best” modelling scheme for multiphase systems. In Sect. 2.8, some conclusions are drawn about the subject of modelling methodologies.

## 2.2 The Empirical Approach

The empirical approach proceeds as follows:

- (1) *Data collection*. A large number of data points are collected, for example, for the pressure gradient ( $dp/dz$ ), for a range of mass flux, quality, physical properties and tube orientation and diameter.
- (2) *Correlation*. Empirical (or semi-empirical) relationships are developed between the *dependent* variables (pressure gradient ( $dp/dz$ ) or pressure drop  $\Delta p$ , for instance) and the *independent* variables (mass flow, quality, geometry and fluid physical properties).
- (3) *Application*. The correlations developed are then applied in hand and computer calculations to predict the design variables. Since the correlations are largely empirical, they are insecure outside the range of data which they cover even at

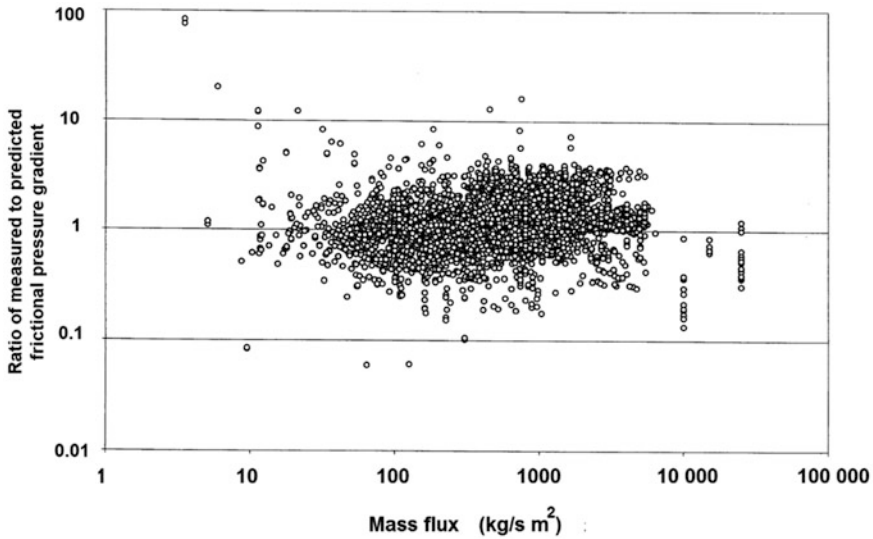


**Fig. 2.3** Comparison of experimental data with the “best” correlation selected for each group of data (ESDU 2002)

steady state. For lack of a better alternative, empirical correlations are often, however, applied also to transient conditions, where they may not be successful (an example is given in Sect. 2.4.4).

An illustration of the errors associated with empirical models is amply provided by an exercise carried out by the former Engineering Sciences Data Unit in the UK (ESDU 2002) on pressure gradient in horizontal two-phase gas–liquid flow. A data bank of 6453 experimental data points for pressure gradient was assembled. This database covered a wide range of physical properties (though with a natural preponderance of low-pressure, air–water data). The database was compared with ten published pressure gradient correlations. The comparisons were grouped into bands of mass flux and quality and the best correlation identified for each respective band. Comparison of the data with these “best” correlations is shown in Figs. 2.3 and 2.4.

Figure 2.3 plots the ratio of measured to predicted frictional pressure gradient as a function of mass flux and it will be seen that in a few cases errors of more than a factor of ten may occur, though the preponderance of the data is (as would be expected) in better agreement than that. Figure 2.4 shows the distribution of errors which essentially gives the same message. The ESDU publication gives methods of assessing the uncertainties in the use of these empirical correlations and, within the range covered by the data base, gives the expected confidence level in a range around the central prediction. The designer is therefore able to make an assessment of the uncertainty (which may be large) and to consider how it affects the system design.

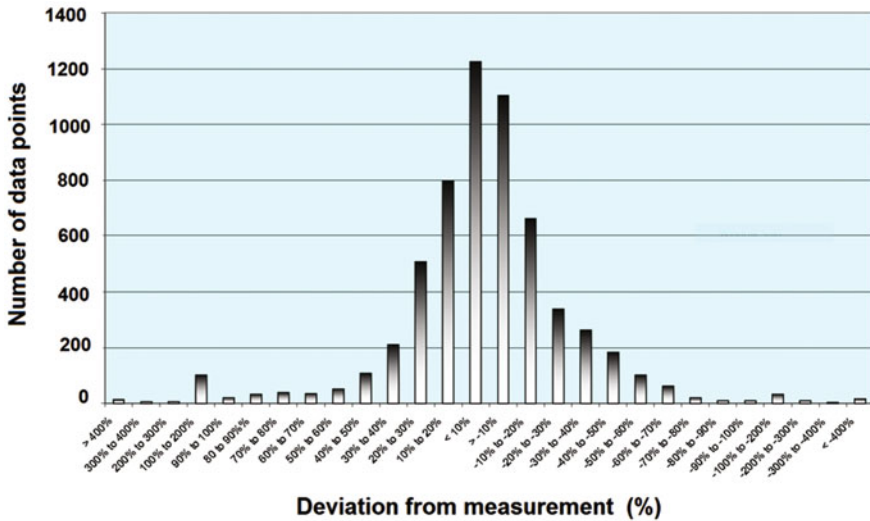


**Fig. 2.4** Distribution of errors in comparisons of predicted and measured values of pressure drop in vertical pipes (ESDU 2002)

The relative failure of empirical correlations for pressure drop, void fraction, etc. has led to the search for improved models and these will be reviewed below. However, it should be stressed that the “improved” models do not necessarily give better results than do the empirical correlations.

The inaccuracies in empirical correlations arise because of a number of factors<sup>1</sup>:

- (1) The experimental data may itself be in error. Measurements in gas–liquid systems are quite difficult but, with adequate attention to detail, one would have expected maximum inaccuracies in measurement of the order of 10–20%.
- (2) The correlation form may be unsuitable. Even with the existence of many adjustable constants, if the form is not adequate, then a good data fit will not be possible.
- (3) The data may be basically uncorrelatable. Factors here include the following:
  - (a) Not all the relevant parameters may be known, particularly local physical properties.
  - (b) There may be unrecognised effects. For example, surface tension can have a large effect on pressure gradient and is hardly ever taken full account of in correlations.
  - (c) The flow may not have reached hydrodynamic equilibrium. In single-phase flows, pressure gradient becomes relatively constant after typically ten tube diameters. In gas–liquid two-phase flow, reaching constant values of

<sup>1</sup>The following discussion is mainly directed to the accuracy of the pressure gradient; similar considerations apply, however, in all other areas.

- pressure gradient may take many hundreds of diameters. Experimental data are rarely obtained under these conditions and, in any case, changes in pressure may occur which give rise to expansion of the gas phase and changes in the gas velocity and hence pressure gradient. In this context, it has been found that approximately constant values of pressure gradient are obtained at *fixed outlet pressure* after several hundred diameters. Thus, even with adiabatic flows, the pressure gradient data may contain significant errors due to lack of equilibrium. Moreover, with diabatic (evaporating or condensing) flows, the potential equilibrium value is in itself changing along the channel and equilibrium conditions rarely pertain in such cases.
- (d) A starting assumption in many calculations is that the phases are in thermodynamic equilibrium. However, this is patently not so in systems with heat transfer where bubbles may exist in the presence of bulk liquid sub-cooling and droplets may exist in the presence of bulk vapour superheat.

It is in the context of the non-equilibrium situations that the real benefits of improved modelling are likely to accrue.

### ***2.2.1 The Empirical Approach Versus Phenomenological Modelling***

As we have shown above, it is clear that the various two-phase flow and boiling heat transfer variables of interest, such as the pressure gradient, the void fraction, the heat transfer coefficient, etc., will depend on the particular flow regime. Thus, in principle, one should model each flow regime separately. This is indeed often done; flow-regime-dependent modelling becomes a necessity if high prediction accuracy is needed; for example, in calculating phenomena taking place in pipelines. When flow-regime-specific models are used, one can “mechanistically” take into consideration the particularities of each regime. However, one drawback of the flow-regime-oriented approach is that one must first predict the prevailing flow regime before undertaking any calculation; this is not always easy. Moreover, the calculation procedure is also considerably lengthened and complicated if many flow regimes can take place.

The alternative approach often used is to largely ignore the flow regimes and derive methods (most often empirical correlations) covering all flow regimes continuously. When the variables used as inputs in the correlations are the same as the ones used in determining the flow regime, such methods can be successful. For example, if mass flux and flow quality are the two variables determining the flow regime (they are not the only ones...), then a correlation of the frictional pressure gradient in term of these two variables has the potential of inherently taking into account the prevailing flow regime.



## 2.3 Phenomenological Modelling

If one looks at Figs. 2.1 and 2.2, it seems obvious that a flow in the bubble flow regime will behave quite differently to one which is in the annular flow regime. In spite of this, empirical correlations often do not take particular account of regimes, and this must be one of the main reasons for their relative failure. In the *phenomenological* approach, the calculations are made for specific flow regimes; this presents a new problem of course, which is the identification of which flow pattern applies for the set of conditions of interest, as already mentioned. Empirical correlations (in the form of flow regime maps, etc. discussed in Chap. 4) exist for flow regime transitions, but these, too, often lack generality and phenomenological modelling is also used in the context of the flow pattern transitions themselves. Thus, the steps for a given flow regime modelling are as follows:

- (1) Observations and detailed measurements are made not only of global parameters such as pressure drop and void fraction, but also of local parameters such as film thickness and entrainment in annular flow, bubble size and bubble distribution in bubbly flow, slug length and slug frequency in slug flow, etc.
- (2) On the basis of the measurements and observations made, physical models of theoretical or semi-theoretical type are formulated to describe the phenomena; these are sometimes called *mechanistic models*.
- (3) The local models are then integrated to achieve a system description, which may notably take account of hydrodynamic and thermodynamic non-equilibrium by modelling the evolution of the flow along the channel.

### 2.3.1 Example: Case of Annular Flow

By way of example, consider the case of annular flow as illustrated in Fig. 2.5.

In order to predict the important system variables (pressure gradient, local phase contents, heat transfer coefficients and critical heat flux) it is necessary to predict the local film and droplet flow rates (e.g. the film flow rate becomes zero at the critical heat flux or dryout condition). The essential components of the phenomenological model for annular flow are as follows:

- (1) Establishment of the local film flow rate ( $\dot{M}_{LF}$ , kg/s). This is done by applying the equation:

$$\frac{d\dot{M}_{LF}}{dz} = P(D - E - q''/h_{LG}) \quad (2.3.1)$$

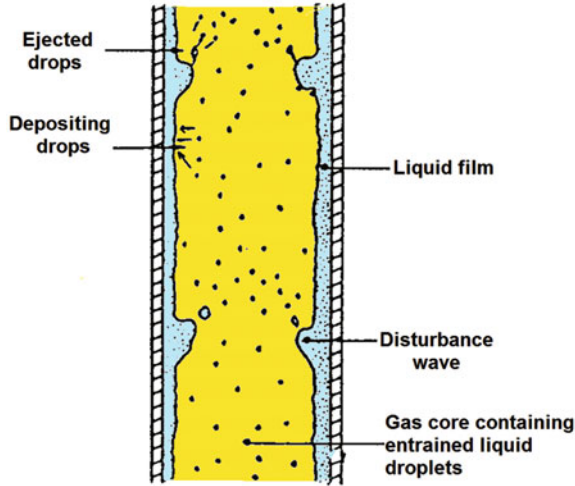


**Fig. 2.5** Schematic illustration of annular flow

where  $P(m)$  is the channel periphery,  $D$  is the rate of deposition of droplets,  $E$  is the rate of entrainment of droplets per unit peripheral area ( $\text{kg/m}^2\text{s}$ ),  $q''$  is the wall heat flux and  $h_{LG}$  is the latent heat of vaporization. This equation is integrated along the channel starting from a given initial or boundary condition to give the film flow rate downstream, at any point. A typical boundary condition would be the fraction entrained at the onset of annular flow; for evaporating flows, the initial condition for film flow rate corresponds to the onset of annular flow. There is a difficulty in providing an accurate value of the initial condition for film flow rate (or entrainment) but, for long enough channels, the initial condition may not be too significant as there will be sufficient time to reach equilibrium between entrainment and deposition.

- (2) If the film flowrate is known, then local values of film thickness and wall shear stress (frictional pressure gradient) can be obtained by combining two relationships as follows:
  - (a) The *triangular relationship* which links film thickness  $\delta$ , interfacial shear stress  $\tau_i$ , and film flowrate. The interfacial shear stress  $\tau_i$  is related to pressure gradient  $dp/dz$  and the triangular relationship can be expressed in the form

$$\dot{M}_{LF} = \dot{M}_{LF}(\delta, \tau_i) = \dot{M}_{LF}(\delta, dp/dz). \quad (2.3.2)$$

The relationship implicit in Eq. (2.3.2) can be obtained by determining the velocity profile and integrating this profile through the film.

- (b) The interfacial shear stress  $\tau_i$  is affected by interfacial waves and, of course, by the gas core velocity. It is conveniently expressed in terms of an interfacial friction factor  $f_i$  which has been found to be approximately a function only of  $\delta/D$  where  $D$  is the tube diameter. This relationship implies that the effective roughness of the interface depends only on the film thickness for a given tube diameter and this implies geometrical similarity between the waves on the interface for a given film thickness, which is confirmed by experimental measurements.

Annular flow modelling has been widely applied and is particularly useful in predicting the onset of dryout. Typical dryout predictions using this kind of model are illustrated in Fig. 2.6. Dryout occurs when the flow rate of the liquid film on the wall goes to zero.

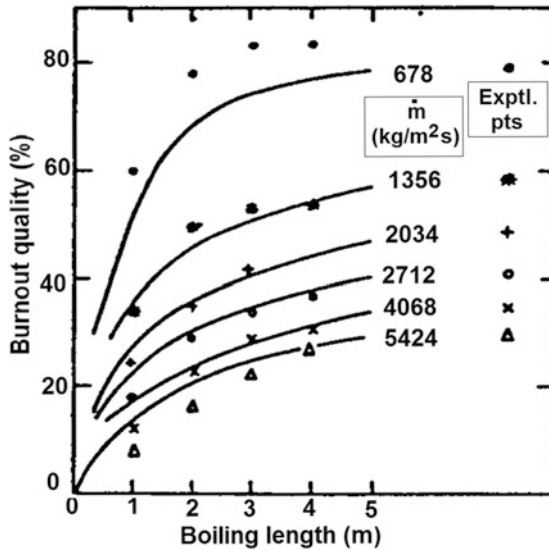


**Fig. 2.6** Prediction of dryout for uniformly heated tubes (continuous lines) and comparison with experimental data (points)—water flow at 70 bar, subcooled inlet condition (Whalley et al. 1974, 1978). Reprinted from Whalley et al. 1974 with permission from Begell House, Inc

## 2.4 Multi-fluid Models and One-Dimensional Conservation Equations

As mentioned above, the formulation of the two-phase-flow problem that would have required the description of the evolution in time of the fields (pressure, velocity, temperature, etc.) for each phase, together with a prediction of the geometry of the interfaces, is generally impractical. The often chaotic flow fields must be treated in terms of statistical, average properties. There are two general approaches, the *two-fluid*, or more generally the *multi-fluid approach* and the *mixture formulation*.<sup>2</sup> A simple presentation of the two-fluid approach will be given in this section. The basis of the method is to write conservation equations for each phase and to include in these equations terms which represent the interaction between the phases.

The two-fluid (or more generally, the multi-fluid) formulation is an *interpenetrating media* approach to the problem: each phase is present at every point, but with a given fractional presence time or frequency or probability, which happens to be the local void fraction. In reality, the phases interact with one another at the *interfaces* separating them. If the gas, for example, has a higher velocity than the liquid, it will create a shear force (a drag force) acting on the liquid at the interface. An equal drag force of opposite sign will act on the gas. This mutual interaction at the interface can be described as an *interfacial momentum exchange*. When the phases exchange energy and mass, there are also *interfacial energy* and *mass exchanges*.

In the interpenetrating media approach, the interfacial transfers are modelled as interfacial terms acting on each phase to explicitly take them into consideration. We write two sets of phase conservation equations (one mass, momentum and energy conservation equation for each phase) in terms of phase-average properties. The dynamics of the interactions between the two phases are described by *closure laws* governing the interfacial mass, momentum and energy exchanges.

When two fluids are used, this approach results in the so-called “six-equation models”. If additional fluids or fields are used, one gets additional equations. For example, if one considers two liquid fields—droplets and film on the wall—and the gas, one gets nine equations. No particular assumptions are made regarding, for example, thermal equilibrium or the velocity ratio; these are obtained naturally from the solution of the set of conservation equations; the phases interact *dynamically* according to the interfacial exchange laws specified.

Starting from the two-fluid formulation, if the phase conservation equations are added together, the interfacial exchange terms cancel out and we end up with three

---

<sup>2</sup>We recall here what was discussed in Chap. 1 regarding the term *mixture* that is most of the time used to denote the two (or more) phases flowing together and does not necessarily imply that these are intimately *mixed*.

*mixture conservation equations* that will be discussed next. In this case, instead of specifying closure laws for the interfacial exchanges, we must specify, for example, how the void fraction or the temperatures of the two phases vary as a function of the quality obtained from the energy equation. We may specify, for instance, a certain value of the velocity ratio, or a velocity ratio that is function of the local quality, etc. Another example would be to “force” one of the phases or both to remain saturated, i.e. to specify phase temperatures that are functions of the local pressure only. Dynamic, thermal interaction of the phases does not take place, however, in this case; the relative behaviour of the phases and the development of the mixture have been prescribed externally and a priori.

The choice between the two alternative approaches depends on the nature of the problem to be solved. The full six-equation model might be needed, for example, for calculating the evolution of the mixture during a fast transient during which strong departures from equilibrium are expected to occur. Slower transients during which there is more time to reach equilibrium may be adequately described by a mixture model.

In the simplest possible mixture model, the *homogeneous equilibrium model* (HEM) equal phase velocities and thermal equilibrium between the phases is assumed.<sup>3</sup>

Local, instantaneous conservation equations can be derived rigorously and then averaged over the entire cross-sectional area of a duct surrounded by a wall, to arrive at instantaneous, space-averaged equations. These can then be time (or ensemble) averaged to arrive at *space and time-averaged equations* (e.g. Delhayé 1981; Ishii and Mishima 1984, Lahey and Drew 1988; Nigmatulin 1979). These derivations will be discussed in more detail in another volume. Here, we will proceed with a more intuitive and simplified derivation of the space and time-averaged equations. This derivation, in spite of being rather primitive, yields equations that have the form and contain practically all the terms obtained from the much more sophisticated derivations mentioned above; they will be useful for the needs of this volume.

### 2.4.1 Simple Derivation of Two-Fluid Conservation Equations

The equations are derived below in a simplified manner (see, e.g. Zuber 1967; Yadigaroglu and Lahey 1976) with reference to a simple flow configuration (in this case annular or stratified flow) where the two phases flow separately, as shown in

---

<sup>3</sup>The term “separated flow” is often used loosely to denote two-phase flows where the two phases have different average velocities. This distinguishes such flows from the *homogeneous* ones, where the phases have the same average velocity; such flows may strictly speaking not be homogeneous at all.



### Mass Continuity

With reference to Fig. 2.7, a notable difference from the single-phase flow formulations is the presence now of the interfacial mass transfer term. Mass continuity for phase  $k$  becomes

$$\frac{\partial}{\partial t} [\langle \rho_k \varepsilon_k \rangle] + \frac{1}{A} \frac{\partial}{\partial z} [\langle \rho_k \varepsilon_k u_k \rangle A] = \Gamma_k \quad k = L, G, \quad (2.4.1)$$

where  $\Gamma_k$  is the volumetric mass transfer rate *into* phase  $k$  (it has units of  $\text{kg/m}^3\text{s}$ ). In case of boiling flow, for example,  $\Gamma_G$  is the rate of vapour generation per unit volume. The first term of the equation above represents the rate of change of mass within the control volume, while the second term is the net convective mass flux into the control volume, as the reader can confirm by examining the various terms in Fig. 2.7. Since there is no mass stored at the interface,

$$\Gamma_L + \Gamma_G = 0,$$

which is the so-called *jump condition* for mass conservation at the interface. We can define

$$\Gamma \equiv \Gamma_G = -\Gamma_L. \quad (2.4.2)$$

### Momentum Conservation

The assumption was made here that the pressure is uniform across the flow area and equal in both phases. This assumption is sometimes justified by the observation that radial pressure differences are usually small and in most cases non-measurable; it is not *always* true, however, as already mentioned. Momentum conservation for phase  $k$  is written as

$$\begin{aligned} & \frac{\partial}{\partial t} [\langle \rho_k \varepsilon_k u_k \rangle] + \frac{1}{A} \frac{\partial}{\partial z} [\langle \rho_k \varepsilon_k u_k^2 \rangle A] \\ &= -\langle \varepsilon_k \rangle \frac{\partial p}{\partial z} + g \langle \rho_k \varepsilon_k \rangle \cos \theta - \frac{P_{wk} u_{wk}}{A} - \frac{P_i \tau_i}{A} + u_i \Gamma_k. \end{aligned} \quad (2.4.3)$$

The first term on the left is again the rate of change of momentum within the control volume, while the second one is the net momentum flux term. The terms on the right are the forces acting on phase  $k$ : the first term is the net pressure force acting on phase  $k$ —it includes contributions due to variable duct area and to variable phase area fraction along the duct. The second term is the gravity force, where  $\theta$  is the angle between the positive  $z$  direction and the acceleration of gravity, Fig. 2.7.

The shear stresses acting on the phase at the wall and at the interface are denoted by  $\tau_{wk}$  and  $\tau_{ik}$ , respectively. The part of wall perimeter wetted by phase  $k$  is  $P_{wk}$ , while  $P_i$  is the interfacial perimeter. The last term represents the momentum addition into phase  $k$  by mass exchange at the interface; as mass crosses the

interface and enters the other phase, it carries with it its original momentum. The mass entering phase  $k$  has a velocity  $u_i$  characteristic of the interface.

Considering the momentum exchanges taking place at the interface (i.e. the jump condition for momentum exchange), we must have

$$\tau_{iL} + \tau_{iG} = 0,$$

and we can define

$$\tau_i \equiv \tau_{iG} = -\tau_{iL}. \quad (2.4.4)$$

### Total Enthalpy Conservation

Defining the total enthalpy of phase  $k$ , i.e. the sum of the intrinsic enthalpy  $h_k$ , and of the kinetic and potential energies by

$$h_k^0 = h_k + \frac{u_k^2}{2} - gz \cos \theta,$$

we can write

$$\begin{aligned} & \frac{\partial}{\partial t} [\langle \rho_k \varepsilon_k h_k^0 \rangle] + \frac{1}{A} \frac{\partial}{\partial z} [\langle \rho_k \varepsilon_k h_k^0 u_k \rangle A] \\ &= q_k''' \langle \varepsilon_k \rangle + \frac{q_{ik}'' P_i}{A} + \frac{q_{wk}'' P_{hk}}{A} + \Gamma_k h_{ik}^0 + \langle \varepsilon_k \rangle \frac{\partial p}{\partial t} - \zeta_k \frac{P_i}{A} \tau_i u_i, \end{aligned} \quad (2.4.5)$$

with  $\tau_i$  given by Eq. (2.4.4).

The first term on the right is the internal heat generation in phase  $k$  due to a volumetric source  $q_k'''$ . The second and third terms are the sensible heat inputs from the interfacial perimeter  $P_i$  and from the heated portion of the perimeter wetted by phase  $k$ ,  $P_{hk}$ . The fourth term accounts for energy addition to phase  $k$  due to interfacial mass transfer;  $h_{ik}^0$  is the specific total enthalpy characteristic of this exchange. The fifth term,  $\langle \varepsilon_k \rangle \partial p / \partial t$ , accounting for the reversible work due to expansion or contraction of the phases should have been written as

$$-\frac{p}{A} \frac{\partial}{\partial t} (\langle \varepsilon_k \rangle A).$$

Using, however, the identity  $\partial(ab)/\partial t = a \cdot \partial b / \partial t + b \cdot \partial a / \partial t$ , we obtain

$$-\frac{p}{A} \frac{\partial}{\partial t} (\langle \varepsilon_k \rangle A) = -\frac{1}{A} \frac{\partial}{\partial t} (p \langle \varepsilon_k \rangle A) + \frac{1}{A} (A \langle \varepsilon_k \rangle) \frac{\partial p}{\partial t}. \quad (2.4.6)$$

The second term on the right side is the one appearing in Eq. (2.4.5). Moreover, the first  $\partial/\partial t$  term on the left side of Eq. (2.4.5) should have contained the internal energy  $e_k$ , not the enthalpy  $h_k$ . However, it has been combined with the  $\partial p / \partial t$  term on the right side as follows. Expanding



$$\frac{\partial}{\partial t} [\langle \rho_k e_k^0 \varepsilon_k \rangle] = \frac{\partial}{\partial t} \left[ \left\langle \rho_k \varepsilon_k \left( e_k^0 + \frac{p}{\rho_k} - \frac{p}{\rho_k} \right) \right\rangle \right] = \frac{\partial}{\partial t} [\langle \rho_k \varepsilon_k h_k^0 \rangle] - \frac{\partial}{\partial t} \left[ \left\langle \rho_k \varepsilon_k \frac{p}{\rho_k} \right\rangle \right]$$

and moving the second term to the right side of Eq. (2.4.5) where we combine it with the first term on the right side of Eq. (2.4.6), we have

$$-\frac{1}{A} \frac{\partial}{\partial t} [p \langle \varepsilon_k \rangle A] + \frac{\partial}{\partial t} [\langle \varepsilon_k \rangle p] = -\frac{A}{A} \frac{\partial}{\partial t} (p \langle \varepsilon_k \rangle) - (\langle \varepsilon_k \rangle p) \frac{\partial A}{\partial t} + \frac{\partial}{\partial t} [\langle \varepsilon_k \rangle p] = 0,$$

provided that the flow area is time independent.

The very last term of Eq. (2.4.5) is related to the interfacial energy dissipation. Although such a term does not appear when the *mixture* is considered, the term shows up in the *phase* energy equations, signifying that the dissipation energy created at the interface is distributed in a certain way, specified by  $\zeta_k$ , between the two phases. We must have

$$\zeta_L + \zeta_G = 0 \quad \text{or} \quad \zeta \equiv \zeta_G = -\zeta_L.$$

The jump condition for energy conservation will be given and discussed below.

### 2.4.2 Practical Set of Two-Fluid Equations

Inspection of the conservation equations derived above reveals the presence of cross-sectional averages of products such as  $\langle \rho_k \varepsilon_k \rangle$ ,  $\langle \rho_k \varepsilon_k u_k \rangle$  and  $\langle \rho_k \varepsilon_k h_k u_k \rangle$ . Within the framework of the one-dimensional theory presented here, we would like to deal with cross-sectionally averaged variables only, e.g.  $\langle u_k \rangle_k$ . It is evident that the averages of products of several variables cannot be evaluated and replaced by the product of their averages unless the cross-sectional *distributions* of these variables (e.g. the phase velocities  $u_k$  and enthalpies  $h_k$ ) are known. Such information is not, however, included in the one-dimensional treatment; it was essentially “lost” during the averaging process; at most it can be provided externally, from knowledge about these distributions obtained by other means.

The angle brackets for the double products containing the void fraction can be “opened” (i.e. the average of the product replaced by the product of averages) using the relationship derived in Chap. 1, Eq. (1.7.8),

$$\langle \varepsilon_k f_k \rangle = \langle \varepsilon_k \rangle \langle f_k \rangle_k,$$

and defining and using an appropriate cross-sectional-average value of the density. This cannot be done, however, for the products of three or four variables.

Regarding the triple products, if the density of a phase is sufficiently constant over the cross section, it can be taken again out of the angle brackets. The constant-density assumption may be an excellent approximation for the liquid, but it may not be always adequate for the gas, for example, in the presence of strong radial temperature gradients. Ignoring the density variations, the remaining double products with the void fraction ( $\langle \varepsilon_k u_k \rangle$  and  $\langle \varepsilon_k h_k \rangle$ ) can then be “opened.”

Finally, there is a fundamental difficulty with the products of four variables, e.g.  $\langle \rho_k \varepsilon_k u_k^2 \rangle$ . If the velocity and enthalpy profiles can be evaluated or guessed independently, then one can use *correlation coefficients*  $C$  to “open the angle brackets”, for example, to write

$$\langle \rho_k h_k u_k \rangle = C \langle \rho_k \rangle_k \langle h_k \rangle_k \langle u_k \rangle_k.$$

If the values of such correlation coefficients are close to unity (as in the case of single-phase turbulent flow where the velocity profile is quite flat), this poses no great problems. We will assume that all correlation coefficients are equal to one in the following treatment.

Terms resulting from the variation of the pressure over the cross section are not included, as already mentioned (the virtual mass terms, for example). The terms dealing with viscous dissipation at the interfaces are also usually ignored. With these simplifications, and using the definitions of  $\Gamma$ ,  $\tau_i$ , etc. given above, the two-fluid conservation equations take the following practical form:

Mass Continuity

$$\frac{\partial}{\partial t} [\rho_L \langle 1 - \varepsilon \rangle] + \frac{1}{A} \frac{\partial}{\partial z} [\rho_L \langle 1 - \varepsilon \rangle \langle u_L \rangle_L A] = -\Gamma \quad (2.4.7)$$

$$\frac{\partial}{\partial t} [\rho_G \langle \varepsilon \rangle] + \frac{1}{A} \frac{\partial}{\partial z} [\rho_G \langle \varepsilon \rangle \langle u_G \rangle_G A] = \Gamma. \quad (2.4.8)$$

Momentum Conservation

$$\begin{aligned} & \frac{\partial}{\partial t} [\rho_L \langle 1 - \varepsilon \rangle \langle u_L \rangle_L] + \frac{1}{A} \frac{\partial}{\partial z} [\rho_L \langle 1 - \varepsilon \rangle \langle u_L \rangle_L^2 A] \\ &= -\langle 1 - \varepsilon \rangle \frac{\partial p}{\partial z} + g \rho_L \langle 1 - \varepsilon \rangle \cos \theta - \frac{P_{wL} \tau_{wL}}{A} + \frac{P_i \tau_i}{A} - u_i \Gamma \end{aligned} \quad (2.4.9)$$

$$\begin{aligned} & \frac{\partial}{\partial t} [\rho_G \langle \varepsilon \rangle \langle u_G \rangle_G] + \frac{1}{A} \frac{\partial}{\partial z} [\rho_G \langle \varepsilon \rangle \langle u_G \rangle_G^2 A] \\ &= -\langle \varepsilon \rangle \frac{\partial p}{\partial z} + g \rho_G \langle \varepsilon \rangle \cos \theta - \frac{P_{wG} \tau_{wG}}{A} - \frac{P_i \tau_i}{A} + u_i \Gamma. \end{aligned} \quad (2.4.10)$$

## Total Enthalpy Conservation

$$\begin{aligned} & \frac{\partial}{\partial t} [\rho_L(1-\varepsilon)\langle h_L^0 \rangle_L] + \frac{1}{A} \frac{\partial}{\partial z} [\rho_L(1-\varepsilon)\langle h_L^0 \rangle_L \langle u_L \rangle_L A] \\ &= q_L'''(1-\varepsilon) + \frac{q_{iL}'' P_i}{A} + \frac{q_{wL}'' P_{hL}}{A} - \Gamma h_{iL}^0 + (1-\varepsilon) \frac{\partial p}{\partial t} \end{aligned} \quad (2.4.11)$$

$$\begin{aligned} & \frac{\partial}{\partial t} [\rho_G \langle \varepsilon \rangle \langle h_G^0 \rangle_G] + \frac{1}{A} \frac{\partial}{\partial z} [\rho_G \langle \varepsilon \rangle \langle h_G^0 \rangle_G \langle u_G \rangle_G A] \\ &= q_G''' \langle \varepsilon \rangle + \frac{q_{iG}'' P_i}{A} + \frac{q_{wG}'' P_{hG}}{A} - \Gamma h_{iG}^0 + \langle \varepsilon \rangle \frac{\partial p}{\partial t}. \end{aligned} \quad (2.4.12)$$

The symbols have the following meaning:

- $\Gamma$  volumetric mass generation rate (positive for vaporization) [ $\text{kg}/\text{m}^3\text{s}$ ]
- $q'''$  internal heat generation rate in phase k
- $P_i$  “interfacial perimeter”
- $P_{wk}$  wall perimeter wetted by phase k
- $P_{hk}$  heated wall perimeter in contact with phase k
- $q_{ik}''$  interfacial heat flux from the interface into phase k
- $q_{wk}''$  heat flux from the wall into phase k
- $\varepsilon$  the void fraction ( $\varepsilon_G$ )
- $\tau_i$  interfacial shear stress acting on the gas (see Eq. (2.4.4))
- $\tau_{wk}$  shear between wall and phase k
- $u_i$  interface velocity
- $\theta$  angle between positive  $z$  direction and acceleration of gravity

Note that the phase conservation equations listed above have the general form:

$$\frac{\partial}{\partial t} [\rho_k \langle \varepsilon_k \rangle \Psi_k] + \frac{1}{A} \frac{\partial}{\partial z} [\rho_k \langle \varepsilon_k \rangle \langle u_k \rangle_k \Psi_k A] = \text{efflux term} + \text{body source term},$$

where  $\Psi_k$  is 1,  $\langle u_k \rangle_k$  and  $\langle h_k \rangle_k$  for mass, momentum and enthalpy continuity, respectively. In Chap. 4 we will have the opportunity to make use of this set of equations for the simple case of horizontal stratified flow.

### 2.4.3 Closure Laws Required

The set of one-dimensional two-fluid conservation equations given above requires knowledge of the following eight terms governing the exchanges at the interface between the phases and at the wall:

- the volumetric mass exchange rate between the phases,  $\Gamma$
- the wall shear force applied to each phase,  $P_{wL}\tau_{wL}$  and  $P_{wG}\tau_{wG}$

- the interfacial shear force,  $P_i \tau_i$
- the heat supplied from the wall to each phase,  $q''_{wL} P_{hL}$  and  $q''_{wG} P_{hG}$
- the interfacial energy transfer rates,  $q''_{iL} P_i$  and  $q''_{iG} P_i$ .

However, one needs only seven exchange laws, since the interfacial heat fluxes and the mass exchange rate  $\Gamma$  are linked through the following *energy jump condition* at the interface:

$$\Gamma(h_{iG} - h_{iL}) + \frac{P_i}{A}(q''_{iG} + q''_{iL}) = 0, \quad (2.4.13)$$

where  $h_{ik}$  are the enthalpies of the phases at the interface, usually assumed to be at saturation. Contributions from minor terms, such as the kinetic energies and surface tension, were ignored in this jump condition. If one assumes that the interface is saturated, Eq. (2.4.13) yields a simple relationship between mass transfer at the interface, the latent heat of vaporization  $h_{LG}$  and the heat fluxes into the phases:

$$\Gamma h_{LG} + \frac{P_i}{A}(q''_{iG} + q''_{iL}) = 0.$$

Figure 2.8a illustrates this interfacial jump condition. If one considers a control volume enclosing the interface and having an infinitesimal thickness (and therefore no mass or energy storage), Eq. (2.4.13) constitutes an energy balance for this volume. Figure 2.8b shows an application of the jump condition. In the *presence of superheated steam and subcooled liquid* (a possible condition in post-dryout heat

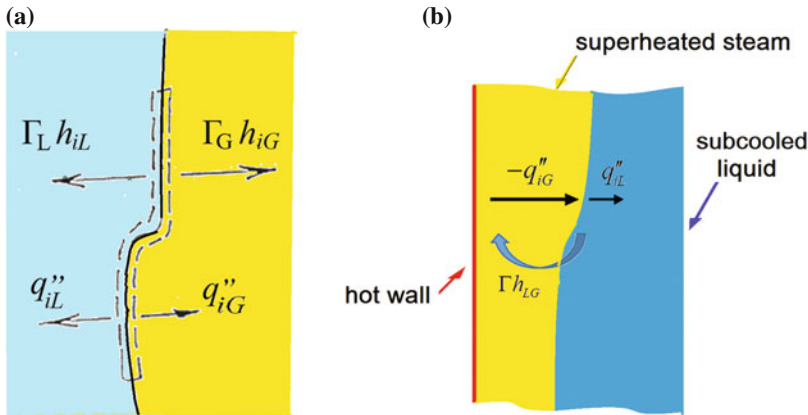


**Fig. 2.8** **a** Control volume used to illustrate interfacial energy exchanges and the jump condition. **b** Application to heat transfer at the interface between superheated steam and subcooled liquid

transfer<sup>5</sup>), there will be heat transfer from the steam to the interface. A fraction  $q''_{iL}$  of the heat flux  $q''_{iG}$  from the interface penetrates into the liquid and is used to heat it up. The remaining fraction produces saturated steam at the interface.

#### 2.4.4 Implementation Difficulties: Application to Horizontal Stratified Flow

The use of multi-fluid modelling implies certain basic assumptions about the averaging of the conservation equations. Although more advanced than a purely empirical approach, the approach still relies on lumped-parameter representation of the quantities. An example is the assignment of a given average velocity to each phase, which is often clearly unrealistic. An example of this would be annular flow where a large fraction of the liquid phase may be entrained as droplets and travelling at a much higher velocity than the liquid film. One could, of course, represent such a situation using a nine-equation model (three equations each for the liquid film, gas core and entrained droplets) but even this may not be sufficient to represent the subtleties of the flow. Lahey and Drew (2001) proposed a *four-field model* that could accurately predict the distribution of the fields of continuous vapour and liquid as well as dispersed vapour and liquid.

The major difficulty with one-dimensional multi-fluid models is that of obtaining sufficiently general relationships for the wall and interface shear terms; these can rarely be directly measured and correlated. An example is discussed here to point at difficulties. The closure laws will be discussed extensively in another volume.

Shaha (1999) made a wide range of measurements on stratified gas–liquid flow which were sufficient to determine  $\tau_{wL}$ ,  $\tau_{wG}$  and  $\tau_i$  independently. Expressing the shear stresses in terms of friction factors, Shaha was able to show that, though the values of  $\tau_{wG}$  were reasonably predicted by existing models, there were large variations between the data and the models for both wall-to-liquid shear stress and interfacial shear stress or friction factors, as illustrated in Figs. 2.9 and 2.10, respectively. It should be noted that the models themselves show large variations in prediction.

For liquid-to-wall shear stress in laminar flows, it is commonly assumed that the friction factor is given by

$$f_L = \frac{16}{\text{Re}_L}, \quad (2.4.14)$$

---

<sup>5</sup>Post-dryout heat transfer refers to the heat transfer regimes that are present after the critical heat flux condition or dryout is reached.

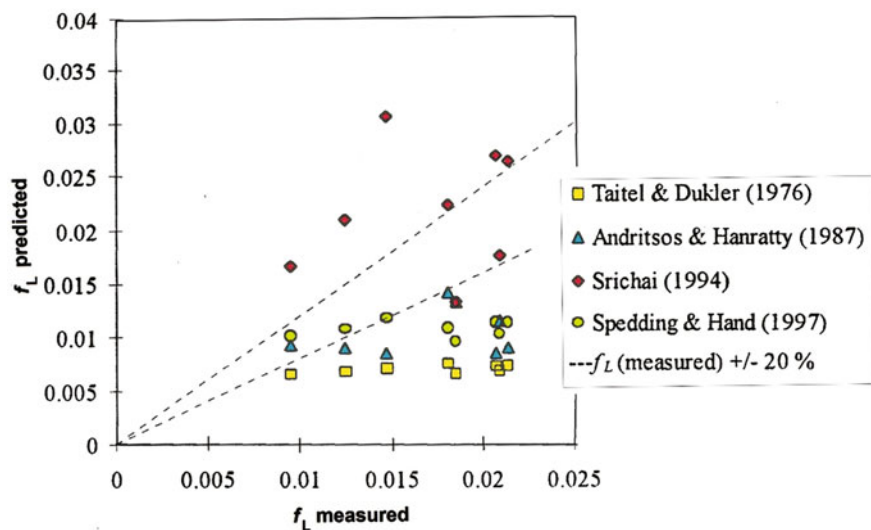


Fig. 2.9 Comparison of measured liquid-wall friction factor with various correlations (Shaha 1999)

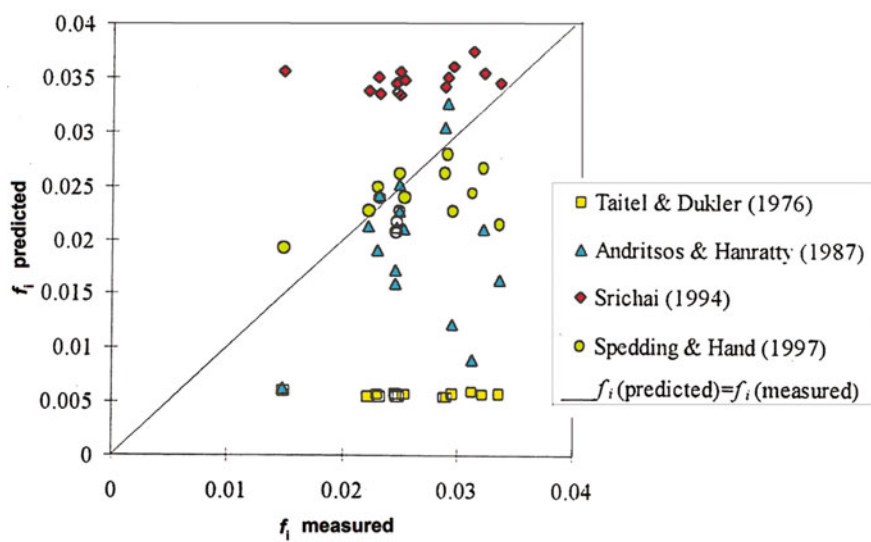


Fig. 2.10 Comparison of experimental interfacial friction factors with various correlations (Shaha 1999)

where the Reynolds number,  $Re_L$  is given by

$$Re_L = \frac{u_L D_H \rho_L}{\mu_L},$$

and  $D_H$  is the hydraulic diameter (which may be defined either with or without inclusion of the interfacial periphery). Calculations on laminar liquid flows with a turbulent gas above them are described by Ng (2002); it was possible to deduce the actual value of the constant in Eq. (2.4.14) from these calculations for a range of conditions. The values obtained can be as low as 4 and approach the classical 16 at the two ends of the liquid fraction spectrum (0 to 1) when the interface is not included in  $D_h$  and are definitively lower (roughly between 2 and 8) when it is included. As expected, the constant approaches the standard value of 16 for a liquid-phase fraction of unity.

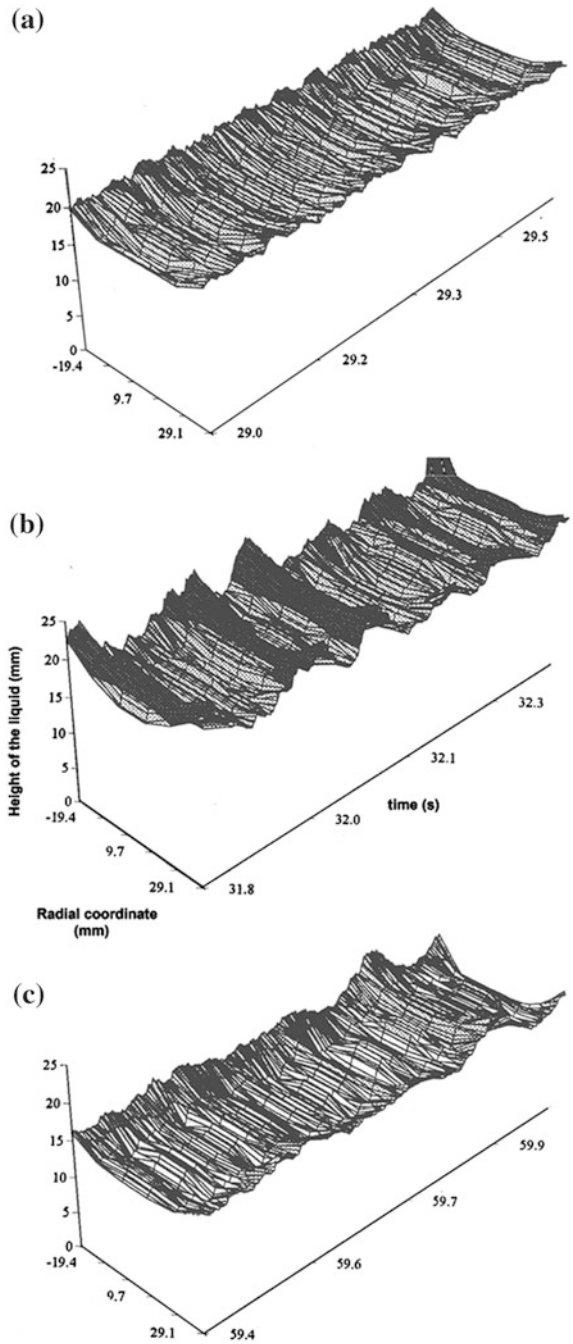
The one-dimensional two-fluid models are commonly also used to calculate transients. This adds further uncertainties to those already shown in Figs. 2.9 and 2.10. Shaha (1999) explored the interfacial structure in stratified flow using multiple twin-wire conductance probes. Figures 2.11a–c typify the results obtained for a transient increase in gas flow rate. Figure 2.11a shows the interfacial configuration before the transient. Figure 2.11b shows the interfacial structure during a transient in which the gas superficial velocity was increased from 5.0 to 6.46 m/s. Eventually, the interface settled down to the configuration shown in Fig. 2.11c at the new value of gas superficial velocity. It is clear from these figures that the interfacial structure during the transient is very different from what would be expected by interpolation between the starting and final values. During the transient, the interfaces are far rougher which implies a much higher value of interfacial shear stress and, indeed, this is borne out by the measurements which suggest that the transient will not be well predicted using steady-state correlations. Such difficulties were already announced in Sect. 2.2.

### 2.4.5 The Drift Flux Model

The presence of two momentum equations in the two-fluid formulation dictates the explicit specification of the momentum exchange terms between the phases. There are, however, difficulties in determining the interfacial closure laws, that most of the time cannot be directly measured, as the example of the preceding section has shown, as well as difficulties in the numerical solution of the equations.

The drift flux model, or DF model for short, (Zuber and Findlay 1967) provides an interesting alternative: the two momentum equations are replaced by a mixture equation where the relative motion between phases is taken into account by a kinematic constitutive relation. The DF model will be discussed in detail in Chap. 5 as it is primarily a way of determining the void fraction. Formulations of the two-phase problems based on the DF concept will be discussed in the volume

**Fig. 2.11** Variation of the interfacial structure in an air–water stratified flow during a transient variation of the gas superficial velocity. **a** steady state with  $U_{sG} = 5.0$  m/s and  $U_{sL} = 0.039$  m/s; **b** the superficial velocity  $U_{sG}$  is now increased to 6.46 m/s; **c** a new steady state is reached with  $U_{sG} = 6.46$  m/s and  $U_{sL} = 0.039$  m/s (Shaha 1999)





dealing with the conservation equations. We can note, however, here that the DF model provides an excellent alternative to the two-fluid model when the phases are closely coupled and “mixed”.

## 2.5 Separated Flow and Mixture Models

As mentioned above, the phase conservation equations may be summed up to yield *mixture conservation equations*. In doing so, we lose *explicit* consideration of the interactions between the phases; as we will see below, the interfacial exchange terms are no longer visible. The interfacial exchanges between the phases can be considered *implicitly* only, e.g. by the empirical correlations describing the mixture.

The forms obtained when the mass, momentum and energy equations, Eqs. (2.4.7) to (2.4.12) are summed up are given below.

### Mass Conservation

$$A \frac{\partial}{\partial t} \langle \rho \rangle + \frac{\partial}{\partial z} (\dot{m} A) = 0, \quad (2.5.1)$$

where the *mixture density*  $\langle \rho \rangle$  and the mixture mass flux  $\dot{m}$  are given by

$$\langle \rho \rangle \equiv \rho_L \langle 1 - \varepsilon \rangle + \rho_G \langle \varepsilon \rangle \quad (2.5.2)$$

$$\dot{m} = \rho_L \langle u_L \rangle_L \langle 1 - \varepsilon \rangle + \rho_G \langle u_G \rangle_G \langle \varepsilon \rangle. \quad (2.5.3)$$

### Momentum Conservation

$$\frac{\partial}{\partial t} \dot{m} + \frac{1}{A} \frac{\partial}{\partial z} A \left( \rho_L \langle 1 - \varepsilon \rangle \langle u_L \rangle_L^2 + \rho_G \langle \varepsilon \rangle \langle u_G \rangle_G^2 \right) = - \frac{\partial p}{\partial z} + g \langle \rho \rangle \cos \theta - \frac{P_w \tau_w}{A}. \quad (2.5.4)$$

Starting from the left, the terms in the momentum equation are identified as the inertial or temporal acceleration, the spatial acceleration, the total pressure gradient, the gravitational pressure gradient and the frictional pressure gradient. One notes that the terms containing the interfacial shear have disappeared now since we are dealing with the mixture. This mixture momentum equation will be used in Chap. 6 as the basis for calculating two-phase pressure drop.

### Total Enthalpy Conservation

$$\begin{aligned} \frac{\partial}{\partial t} \left( \rho_L \langle h_L^0 \rangle_L \langle 1 - \varepsilon \rangle + \rho_G \langle h_G^0 \rangle_G \langle \varepsilon \rangle \right) \\ + \frac{1}{A} \frac{\partial}{\partial z} A \left( \rho_L \langle 1 - \varepsilon \rangle \langle h_L^0 \rangle_L \langle u_L \rangle_L + \rho_G \langle \varepsilon \rangle \langle h_G^0 \rangle_G \langle u_G \rangle_G \right) = q''' + \frac{P_h q_w''}{A} + \frac{\partial p}{\partial t}. \end{aligned} \quad (2.5.5)$$

Again we notice that the interfacial exchanges do not appear any longer in this equation and the heat flux from the wall heats the mixture rather than the phases separately.

In the momentum Eq. (2.5.4), only the momentum flux term (second term) is “different” from the corresponding terms in the single-phase momentum equation. This term can also be written, however, in a “single-phase fluid” form by defining (Meyer 1960) the *momentum density*  $\rho'$  (or specific volume  $v'$ ),

$$\frac{1}{\rho'} \equiv \frac{(1-x)^2}{\rho_L \langle 1 - \varepsilon \rangle} + \frac{x^2}{\rho_G \langle \varepsilon \rangle} \equiv v'. \quad (2.5.6)$$

The mixture *momentum conservation equation* then takes the form

$$\frac{\partial}{\partial t} \dot{m} + \frac{1}{A} \frac{\partial}{\partial z} \left[ \frac{A \dot{m}^2}{\rho'} \right] = - \frac{\partial p}{\partial z} + g \langle \rho \rangle \cos \theta - \frac{P_w \tau_w}{A}. \quad (2.5.7)$$

Regarding the energy equation, we will generally neglect the contribution to the total enthalpy due to kinetic and potential energy, i.e. we will assume that  $h_k^0 \approx h_k$ . Indeed in most problems of thermal hydraulics the changes in kinetic energy and potential energy are very small compared to the changes in enthalpy; this is not true, e.g. in turbomachinery where the kinetic energy of the gas varies very significantly to produce work.

The proper definition of mixture enthalpies can be obtained from the energy equation. Two definitions will be needed since the enthalpy is *volume* or *mass* weighted in the time derivative term (stemming from the rate of change of the *contents* of the infinitesimal control volume), while it is *mass flux* weighted in the enthalpy *flux* (the  $\partial/\partial z$ ) term. Since

$$\rho_L \langle 1 - \varepsilon \rangle \langle u_L \rangle_L \equiv (1-x) \dot{m} \quad \text{and} \quad \rho_G \langle \varepsilon \rangle \langle u_G \rangle_G \equiv x \dot{m},$$

it follows that we must have two mixture enthalpies defined: a new, *mass* weighted  $\bar{h}$  and the conventional, *mass-flow-rate* weighted  $h$ :

$$\bar{h} \equiv \frac{\rho_L \langle 1 - \varepsilon \rangle \langle h_L \rangle_L + \rho_G \langle \varepsilon \rangle \langle h_G \rangle_G}{\langle \rho \rangle} \quad (2.5.8)$$

$$h \equiv (1 - x) \langle h_L \rangle_L + x \langle h_G \rangle_G. \quad (2.5.9)$$

With these definitions, the total enthalpy equation takes the *visually* simple form resembling the single-phase enthalpy equation:

$$\frac{\partial}{\partial t} [\langle \rho \rangle \bar{h}] + \frac{1}{A} \frac{\partial}{\partial z} [A \dot{m} h] = q''' + \frac{P_h q_w''}{A} + \frac{\partial p}{\partial t}. \quad (2.5.10)$$

The equation above shows that, at steady state (i.e. without the  $\partial/\partial t$  term), the enthalpy  $h$  of the mixture at a given point in the channel can be obtained from a simple heat balance. Indeed, by integrating the steady-state form of Eq. (2.5.10) (with the volumetric heating  $q'''$  term “included” in  $q_w''$ ):

$$h(z) - h_{in} = \frac{P_h}{\dot{M}} \int_0^z q_w'' dz = \frac{1}{\dot{M}} \int_0^z q_w' dz, \quad (2.5.11)$$

where  $q_w' = P_h q_w'' + A q'''$  is the total, equivalent, linear heat generation rate.

If one assumes that the two phases are in *thermal equilibrium*, i.e. that their enthalpies are equal to the saturation enthalpies corresponding to the local pressure,

$$h_L = h_{L,sat}(p) \quad \text{and} \quad h_G = h_{G,sat}(p),$$

then one can calculate from Eq. (2.5.9) the local *equilibrium* quality  $x_{eq}$ :

$$x_{eq} = \frac{h - h_{L,sat}}{h_{LG}}, \quad (2.5.12)$$

where  $h_{LG}$  is the heat of vaporization,  $h_{LG} = h_{G,sat} - h_{L,sat}$ .

## 2.6 The Homogeneous Model

If one assumes that the two-phase velocities are equal,  $\langle u_L \rangle_L = \langle u_G \rangle_G$ , then all the equations are very much simplified and one obtains the homogeneous model. Note that no assumption about any other “homogeneity” of the flow is required, the condition  $S = 1$ , is sufficient to derive the homogeneous model conservation equations that look very much like the single-phase conservation equations. The various definitions of the density or specific volume and of the enthalpy of the

mixture that were needed to write the mixture conservation equations for the separated flow model all merge into their unique homogeneous model form

$$\langle \rho \rangle = \frac{1}{\langle v \rangle} = \frac{1}{v_L + xv_{LG}} \quad \text{or} \quad \frac{1}{\langle \rho \rangle} = \frac{1-x}{\rho_L} + \frac{x}{\rho_G}$$

$$\bar{h} = h = (1-x)\langle h_L \rangle_L + x\langle h_G \rangle_G$$

and the homogeneous model conservation equations become

$$A \frac{\partial}{\partial t} \langle \rho \rangle + \frac{\partial}{\partial z} (\dot{m}A) = 0 \quad (2.5.13)$$

$$\frac{\partial}{\partial t} \dot{m} + \frac{1}{A} \frac{\partial}{\partial z} A \left[ \frac{A \dot{m}^2}{\langle \rho \rangle} \right] = - \frac{\partial p}{\partial z} + g \langle \rho \rangle \cos \theta - \frac{\tau_w P_w}{A} \quad (2.5.14)$$

$$\frac{\partial}{\partial t} [\langle \rho \rangle \langle h \rangle] + \frac{1}{A} \frac{\partial}{\partial z} A [\langle \rho \rangle \langle h \rangle] = q''' + \frac{P_h q_w''}{A} + \frac{\partial p}{\partial t}. \quad (2.5.15)$$

For homogeneous flow, the unique mixture velocity is then simply

$$\langle u \rangle = \frac{\dot{m}}{\langle \rho \rangle} = \langle j \rangle. \quad (2.5.16)$$

Another advantage of the homogeneous model, beyond its inherent simplicity, is that when an expression for the quality and consequently for  $\langle \rho \rangle$  is available, and the fluid properties can be considered constant along the channel, the conservation equations can often be analytically integrated (for example, to compute the pressure drop along a channel).

### Example: Computation of the Local Equilibrium Quality and of the Homogeneous Void Fraction

The purpose of this small exercise is to familiarize the reader with the use of the equations derived above, show the ease with which the homogeneous model can produce analytical results and provide a flair for the orders of magnitude. We consider a uniformly heated tube with a length  $L = 10$  m and a diameter of 20 mm, receiving a mass flow rate of 1 kg/s of water (for the 20 mm diameter tube this corresponds to a mass flux of 3183 kg/m<sup>2</sup>s and a velocity of 4.3 m/s) with an inlet subcooling of 30 °C (i.e. 30 °C below the saturation temperature corresponding to the system pressure) and operating at a system pressure of 70 bar (assumed constant along the tube as it should vary little with respect to its absolute value). The total power input to the tube is uniform and amounts to 1 MW, yielding a linear heat input rate  $q' = 100$  kW/m. We will calculate now the variation (along the length of the tube  $z$ ) of the equilibrium quality  $x_{eq}$ , and, under the assumption of homogeneous flow, the specific volume  $v$ , the density  $\rho = \langle \rho \rangle$  of the mixture and the void fraction  $\langle \epsilon \rangle_{hom} = \beta$ .

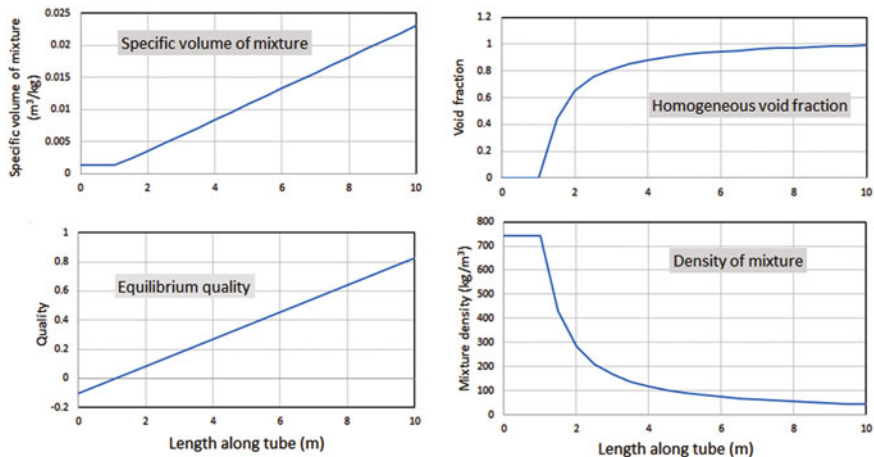


**Fig. 2.12** Variation along the length of a heated tube of the equilibrium quality, of the specific volume and density of the mixture and of the void fraction

Equations (2.5.12) and (2.5.11) allow us to compute the local equilibrium quality  $x_{eq}$

$$x_{eq} = \frac{h(z) - h_{L,sat}}{h_{LG}} = \frac{1}{h_{LG}} \left[ \frac{1}{\dot{M}} \int_0^z q' dz + h_{in} \right] - \frac{h_{L,sat}}{h_{LG}} = \frac{q'z}{\dot{M}h_{LG}} - \frac{\Delta h_{in}}{h_{LG}},$$

where  $\Delta h_{in} \equiv h_{L,sat} - h_{in}$  is the inlet subcooling in terms of enthalpy. The first term on the right side is a dimensionless enthalpy addition and the second the dimensionless inlet subcooling; in both cases the non-dimensionalization is provided by dividing by the latent heat, a fundamental phase change and fluid parameter. Knowing the quality, we can compute the specific volume of the mixture

$$v = v_L + xv_{LG} \text{ with } v_{LG} \equiv v_G - v_L.$$

Clearly,  $\rho = 1/v$ . The homogeneous void fraction is given by Eq. (1.9.10) of Chap. 1 as

$$\beta = \frac{xv_G}{v_L + xv_{LG}}.$$

Figure 2.12 shows the results for the case considered. One notes the linear increases of the quality and of the specific volume (following the linear increase of the quality), the fast drop of the density of the mixture and the corresponding rise of the void fraction that, even at this relatively high pressure, reaches values near unity for qualities above about 0.5.

## 2.7 Computational Multiphase Flow Dynamics

We will introduce in this section summarily these relatively new developments that rely on computational methods to analyse and simulate multi- and two-phase flows. As the purpose, at this point, is to make the reader only aware of their existence, we will limit ourselves to an introduction as these will be covered in other volumes. We will also briefly mention only the extension to 3D of the 1D methods presented above, in particular the two-fluid approach.

Computational Fluid Dynamics (CFD) has been widely applied industrially to single-phase flow problems, but the extension of related methods to multiphase flows is new and at its infancy; the difficulties are much greater. We proposed to label this relatively new discipline Computational *Multi-Fluid* Dynamics or CMFD for short (Yadigaroglu 2003). The CMFD techniques are “CFD like” in the sense that they are based on the well-established bases of Fluid Mechanics, are three-dimensional, consider the turbulence and use computational techniques. In complexity and difficulty, however, they are clearly one step beyond the classical CFD of single-phase flows. As it happened for single-phase flows, detailed numerical CMFD experimentation is again providing an alternative to laboratory investigations in multiphase flow situations.

The computational developments need inputs from new experiments to provide the detailed data necessary to verify the much more detailed computations. Advanced instrumentation needed for future work is discussed in another volume.

### 2.7.1 Treatment of Separated Phases as Single-Phase Flow

We start the discussion with an example where the two phases are treated separately by a single-phase CFD code. Indeed, in general, if the position of the interface is known, and if the distribution of shear stress and pressure can be specified along the interface, then solutions can be obtained which may throw valuable light on the flow behaviour. Results of one such an early calculation (Jayanti and Hewitt 1997) are illustrated in Fig. 2.13, which shows predicted velocity vectors within a disturbance wave in annular flow, based on the use of empirical correlations for the interfacial shear stress. The profile of the interface was *assumed* (and was kept fixed throughout the calculations). The wall was moved at the wave velocity in a direction opposite to the flow so as to keep the shape of the interface fixed, thus permitting a steady-state calculation of the flow field. The geometry and flow conditions specified were typical of those encountered in gas–liquid annular flow. The results showed that the flow in the substrate layer was laminar while that in the disturbance wave region was turbulent, leading to a local enhancement of the transport coefficients.

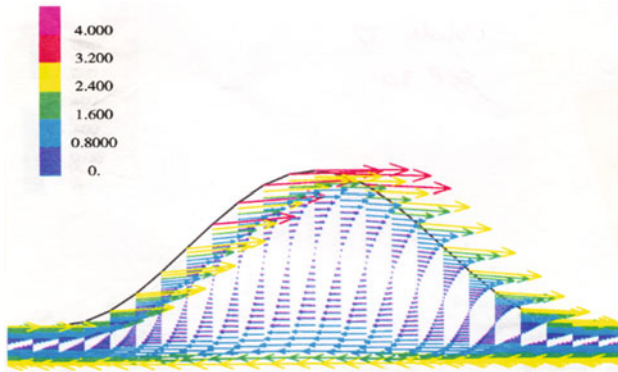


**Fig. 2.13** Predicted velocity vectors in a disturbance wave in annular flow (Jayanti and Hewitt 1997). Note that the view of the wave is considerably foreshortened in the axial direction to allow a better view of the velocity vectors. The velocities are coloured in m/s

### 2.7.2 One-Fluid Formulation with Interface Tracking Versus Two-Fluid Formulations

#### The One-Dimensional, Two-Fluid Model

At this point, it is worth recalling the basic premise of the two-fluid model. The separate phase conservation equations are derived from an averaging procedure that allows both phases to co-exist at any point, according to a certain phase indicator function, or essentially a probability, that is the local instantaneous void fraction, Fig. 2.14. The approach is also referred to as the “interpenetrating media” formulation, a term that reminds us of the basic assumption made. With the two-fluid model, each phase, governed by its own conservation equations, moves and develops independently. The interfacial exchange terms provide the interactions between the phases.

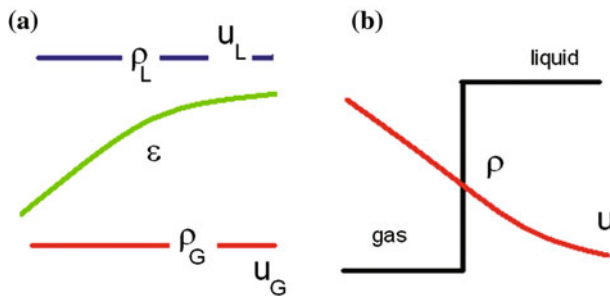


**Fig. 2.14** Two-fluid (left) versus one-fluid (right) formulation; in this case the velocity field is unique but, e.g. the density changes abruptly at the interface

Although the presence of the interfaces *has* been considered during the local averaging process (and led to the definition of the local interfacial area concentration for the inter-phase exchanges), the characteristics of the interfaces (their exact shape and position) are “lost” in the interpenetrating media, formulation. The exact topology of the phases cannot be obtained and consequently the flow regimes cannot really be determined, except by correlation with the average flow conditions. The two-fluid, 1D model cannot tell if, say at a 30% void fraction, the flow is stratified or bubbly. This is fine with many problems, but there are situations where the two phases are sharply separated (at a large scale, such as that of the duct) and an understanding of the situation requires knowledge of the positions of the interfaces. This could be, for example, the case of injection of subcooled water in a pipe with stratified two-phase flow; clearly one needs to know the characteristics of the steam-water interface to estimate the rate of condensation taking place there.

### **Multidimensional Implementation of the Two-Fluid Model and Alternatives**

Some of the limitations mentioned above can be removed by applying the two-fluid model to three-dimensional situations. Indeed, it is possible to write multidimensional equations analogous to the one-dimensional equations described above (e.g. Lahey and Drew 1988; Ishii and Hibiki 2011). Solutions of these equations allow flow fields and phase fraction distributions to be determined. Of course, in three dimensions, the closure challenge is even greater.

For example, the injection of a large bubble from a vent into water and its condensation is a situation where the shape and extent of the liquid–gas interface are important. Although the two-fluid model could, in some way, deal with this vent discharge and similar problems, in practice this is not totally satisfactory. Indeed, one could start the vent flow problem with the volume occupied by gas characterized as a region of void fraction unity, and the liquid volume as a region of void fraction zero. Numerical diffusion will very quickly mix the two phases, however, and the interface will lose its sharpness and disappear. *Interface sharpening methods* (Štrubelj et al. 2009; Gauss et al. 2016) can be used to overcome this problem, but there are better solutions, namely the *Interface Tracking (IT)* methods discussed below.

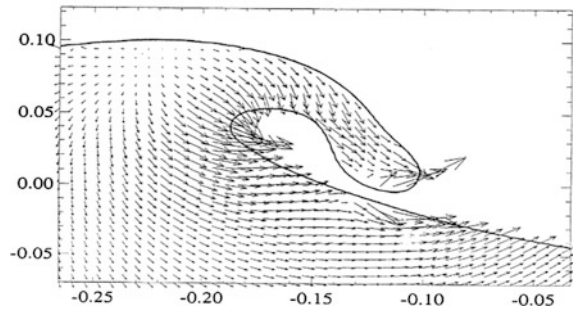
There are also cases where prediction of the location of the phases, leading essentially to the definition of the flow pattern, is needed. Other situations that are good candidates for application of IT methods are those for which the stability of the interface plays an important role: the stability and break-up of jets is a good example.

### **One-Fluid Formulation with Interface Tracking (IT)**

All the IT methods are associated with a “one-fluid” description of the two-phase flow system: while in the interpenetrating media formulation the conservation equations were appropriately averaged (for example, over volume) *for each phase separately*, in the *one-fluid, IT* formulation, the same conservation equations are used for the entire computational domain, but the fluid properties such as density and viscosity vary sharply across the interface as we move from one phase into the other, Fig. 2.14. Thus, the two-phase system is treated as a continuous fluid whose



**Fig. 2.15** Example of the application of the VOF method: prediction of a breaking wave (Chen et al. 1999). Reproduced from Chen et al. 1999 with the permission of AIP publishing



properties vary from those of the liquid to those of the gas over a narrow range of values of a phase-indicating scalar or “colour function” (that is typically given limiting values of 0 and 1 for the two phases). An equation is written for the transport of the scalar with the fluid. Kataoka (1986) discusses the bridge between the two (one- or two-fluid) approaches.

The position of the interface is tracked using a variety of procedures; our purpose is only to mention these here (and refer to some of the related seminal work) as they will be treated in other volumes. Rider and Kothe (1998) and Lakehal et al. (2002) review these methods that can be classified as either Lagrangian or Eulerian according to the way the motion of the interface is tracked.

The most frequently employed Eulerian IT methods are the *Volume-of-Fluid* (VOF) method that is based on the earlier multi-fluid simulations using the so-called *Marker-And-Cell* (MAC) approach (see the classical work of Hirt and Nichols (1981) and a recent implementation by Scardovelli and Zaleski (1999)) and its *Level Set* (LS) variant (Osher and Sethian 1988; Sussman et al. 1994). Figure 2.15 illustrates an early, two-dimensional, VOF computation of a breaking wave.

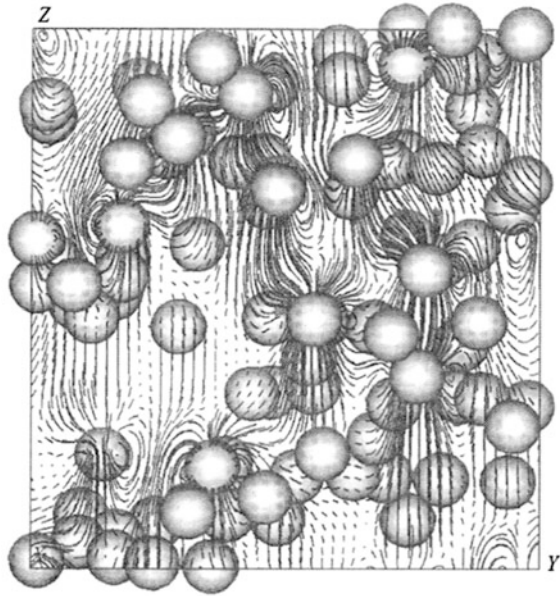
In *Lagrangian or embedded interface methods* (Unverdi and Tryggvason 1992; Tryggvason et al. 2001), particles are typically used to track the motion of the interfaces. The grid that they form can adapt to account for any changes in the interfacial shape. Again, an early application of this method is shown in Fig. 2.16 where the structure of an array of bubbles (originally equally spaced) has been calculated.

The so-called “second gradient method” offers alternative capabilities (Jamet et al. 2001). The relative merits of VOF and LS, as well as other possibilities, are discussed by Rider and Kothe (1998) and Scardovelli and Zaleski (1999).

### 2.7.3 Multiplicity of Scales

System behaviour and the various physical phenomena taking place in the system can sometimes be best addressed at a multiplicity of time and space scales. Let us refer to these as the micro-, the meso- and the macro-scale. For example, an entire

**Fig. 2.16** Application of the front tracking method to the prediction of the motion of a three-dimensional array of bubbles (Bunner and Tryggvason 2002)



large-scale system such as a nuclear plant or a steam generator can be modelled at the macro-scale; a system component may need to be examined at the meso-scale. Local flow in a critical part of a component may need to be addressed at the micro-scale, Fig. 2.17. At each level of the scale hierarchy, the physics of the flow are best amenable to numerical prediction by scale-specific strategies.

Cross-scale interactions (feedback and forward transfer of information) between the micro-, meso- and macro-scales) require merging of the solutions delivered by the scale-specific approaches at each level of the scale hierarchy. As shown in Fig. 2.17, considering the top-down path, the computations at each level provide the boundary conditions needed at the lower levels. On the inverse path, starting from the bottom-up, the computations at each level will deliver the closure laws needed at the higher level. For example, local, detailed CFD computations may deliver the heat transfer coefficient needed to describe the behaviour of a component, and component behaviour will provide the information needed at the system level.

Instances where a full understanding of a situation or phenomenon requires solution of such a “cascade” of problems at various scales with a corresponding panoply and hierarchy of tools were discussed by Yadigaroglu (2005), Yadigaroglu and Lakehal (2003) and Chauliac et al. (2011). For example, for nuclear systems, the behaviour of the entire system is typically obtained using a system code based on the two-fluid approach and operating at macro-scales comparable to the dimensions of the system and its components. Local phenomena, or the behaviour of parts of the system, may be addressed at the meso-scale level, with tools considering smaller scales and more detailed description of phenomena. Finally, one

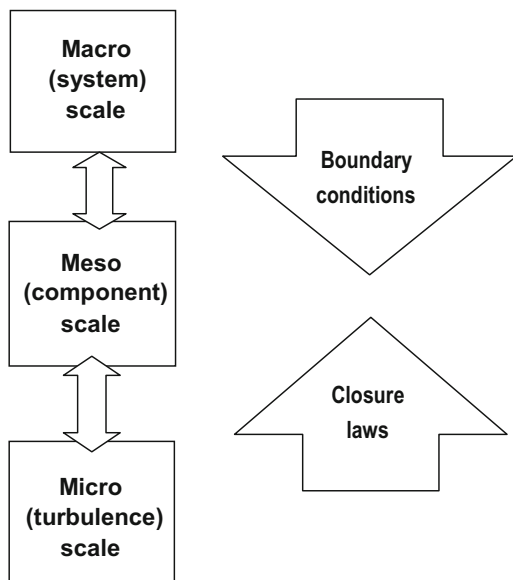


**Fig. 2.17** Multiplicity of scales and transfers of information

may obtain, for example, wall and interfacial momentum, heat and mass transfer laws by performing studies at micro-scales, for example, via *Direct Numerical Simulation* (DNS)<sup>6</sup>; such level of spatial resolution is indeed needed to resolve the gradients determining transfers at the interfaces.

A recent example of advanced VOF simulation *and* of multi-scale computing is given in Fig. 2.18. The study by Ling et al. (2015) proposes a model for atomization simulations, where the large-scale interfaces are resolved by the VOF method and the resulting small droplets by a Lagrangian point-particle model.

### Molecular Dynamics

Pushing the computations and the scales to the infinitesimal level, *Molecular Dynamics*, studying the physical behaviour and movements of atoms and molecules, is the ultimate tool in CFD and CMFD (e.g. Alder and Wainwright 1957; Long et al. 1996). We will only mention here the possibility of investigating phenomena such as the vaporization of an ultra-thin liquid layer on a hot metallic surface by molecular dynamics simulations (e.g. Yi et al. 2002). In this case, the forces acting between all combinations of pairs of wall and fluid molecules are

<sup>6</sup>Contrary to other authors, we do not use the term DNS to characterize all “fully resolved” computations, but apply it only to computations where all the scales of *turbulence* are resolved. In this sense, an exact analytical solution for laminar flow is not a DNS (Yadigaroglu 2005).

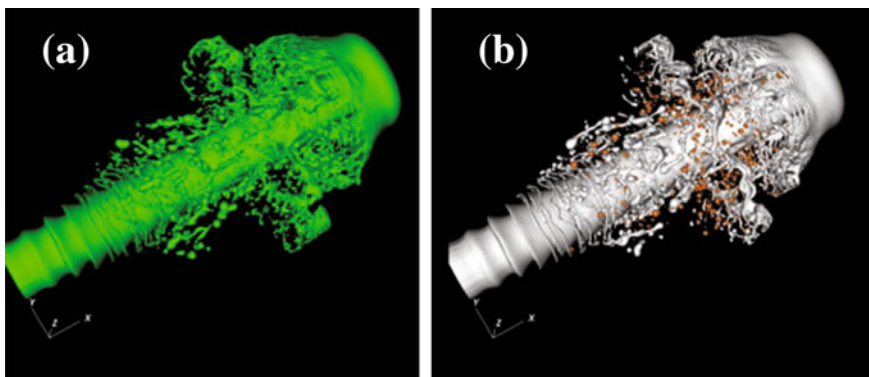


**Fig. 2.18** Example of VOF computations coupled with a particle tracking method to track the small droplets. The figure shows a snapshot of the liquid–gas interface of an atomizing pulsed jet. **a** using fully resolved droplets. **b** using the coupled-model method where the orange droplets are from the tracked ones (Ling et al. 2015)

modelled and the evolution of the system is simulated numerically; the results of Yi et al. (2002) show resemblance to our knowledge of such vaporization events.

#### 2.7.4 DNS of Turbulent Multiphase Flows

Contrary to terminology used by other authors, by Direct Numerical Simulation (DNS), we mean *capturing the entire turbulence spectrum of length and time scales without resorting to modelling* (Yadigaroglu 2003). In two-phase flow, so far, DNS has been primarily applied to study the physics of small particle dispersion using Eulerian–Lagrangian point tracking, or, occasionally, using the Eulerian, two-fluid formulation; as an example, we can cite the bubble-laden mixing layer work by Druzhinin and Elghobashi (2001).

Interface tracking methods, although not limited *in theory* to consideration of turbulence in the fluids by an associated DNS, are *in practice* not adequate for the purpose. Even in Large Eddy Simulation (LES) where the large scales of turbulence are resolved, while the small ones are modelled, the scales still needed for resolving the large scales of turbulence may be much smaller than those of the interfaces. Thus, even rather simple *turbulent* bubbly flows are still often far from DNS. Conducting true DNS studies in multiphase flows has proven, however, possible for certain relatively very simple flow situations, for example, for counter-current gas liquid flows separated by a sheared interface; the latter can be deformable within limits, i.e. without the presence of breaking waves (Fulgosi et al. 2003; Lakehal et al. 2003). As this approach tackles all the physics of the problem without recourse to modelling, this method can be regarded as a true DNS of turbulence in

*multiphase* flow. Such sophisticated techniques are understandably limited to a narrow range of applications, where they can serve as “numerical experiments” for exploring small-scale, turbulence-induced transport phenomena at the interface.

## 2.8 Conclusions

One may make the following general observations about the state of prediction methods in multiphase flow systems:

- The prediction of multiphase systems represents a formidable challenge and great accuracy cannot be expected.
- The widely used empirical models do not predict data outside their range of derivation.
- *Phenomenological* (or *mechanistic*) modelling offers insight into the processes occurring but needs sub-models (e.g. for droplet entrainment and deposition) which may not yet have a secure base.
- Multi-fluid (two-fluid) models provide an elegant framework but are less flexible than phenomenological models. The identification of general closure relationships has proved a difficult goal.
- CFD and CMFD modelling are already a useful research tools, giving insights into flow phenomena. They are far from being readily applicable to all industrial problems.
- Single-phase CFD techniques are mature; their application to large systems is only limited by available computing power. The commercial CFD codes are readily usable in many areas, but specific models need often to be added to consider particular phenomena.
- CMFD techniques can already tackle certain flow regimes. Interface tracking methods such as VOF and level sets are capable of dealing with flows where the interfaces are relatively simple, e.g. stratified flows or wavy annular flows. There are much greater difficulties in dealing with flow regimes presenting complex interfaces, such as churn flows.
- Cascades of computations at different scales are needed to address certain problems.
- DNS and more specifically the future DNS of two-phase flows is likely to be successfully used to investigate microscopic phenomena that are not amenable to experimental observation in the manner of numerical experiments.

Multiphase flow is a diverse and complex subject with many subtleties and a whole variety of solution approaches. We hope that by presenting a whole variety of viewpoints, the richness of the subject will become apparent.

## References

- Alder BJ, Wainwright TE (1957) Phase transition of a hard sphere system. *J Chem Phys* 27(5):1208
- Andritsos N, Hanratty TJ (1987) Influence of interfacial waves in stratified gas-liquid flows. *AIChE J* 33(3):444–454
- Bird RB, Stewart WE, Lightfoot EN (1960) *Transport phenomena*. Wiley, New York
- Bunner B, Tryggvason G (2002) Dynamics of homogeneous bubbly flows. Part 1. *J Fluid Mech* 446:17–52
- Chauliac C, Aragonés JM, Bestion D, Cacuci DG, Crouzet N, Weiss FP, Zimmermann MA (2011) NURESIM—A European simulation platform for nuclear reactor safety: multi-scale and multi-physics calculations, sensitivity and uncertainty analysis. *Nucl Eng Des* 241(9):3416–3426
- Chen G, Kharif C, Zaleski S, Li J (1999) Two-dimensional Navier-Stokes simulation of breaking waves. *Phys Fluids* 11(1):121–133. doi:[10.1063/1.869907](https://doi.org/10.1063/1.869907)
- Delhaye JM (1981) Local instantaneous equations, local time-averaged equations, and composite-averaged equations. In: Delhaye JM, Giot M, Riethmueller ML (eds) *Thermohydraulics of two-phase systems for industrial design and nuclear engineering*. Hemisphere, Washington
- Druzhinin OA, Elghobashi S (2001) Direct numerical simulation of a three-dimensional spatially developing bubble-laden mixing layer with two-way coupling. *J Fluid Mech* 429:23–61
- ESDU (2002) Frictional pressure gradient in adiabatic flows of gas-liquid mixtures in horizontal pipes: prediction using empirical correlations and data base. Engineering Sciences Data Unit, Data Item 01014 (ISBN 1 86246 171 6). ESDU International Ltd, London
- Fulgosi M, Lakehal D, Banerjee S, De Angelis V (2003) Direct numerical simulation of turbulence in a sheared air-water flow with a deformable interface. *J Fluid Mech* 482:319–3457
- Gauss F, Lucas D, Krepper E (2016) Grid studies for the simulation of resolved structures in an Eulerian two-fluid framework. *Nucl Eng Des* 305:371–377
- Hirt CW, Nichols BD (1981) Volume of Fluid method (VOF) for the dynamics of free boundaries. *J Comput Phys* 39:201–225
- Ishii M, Hibiki T (2011) *Thermo-fluid dynamics of two-phase flow*, 2nd edn. Springer, New York
- Ishii M, Mishima K (1984) Two-fluid model and hydrodynamic constitutive relations. *Nucl Eng Des* 82:107–126
- Jamet D, Lebaigue O, Coutris N, Delhaye JM (2001) The second gradient method for the direct numerical simulation of liquid-vapor flows with phase change. *J Comput Phys* 169:624–651
- Jayanti S, Hewitt GF (1997) Hydrodynamics and heat transfer in wavy annular gas-liquid flow: a computational fluid dynamics study. *Int J Heat Mass Transf* 40:2445–2660
- Kataoka T (1986) Local instant formulation of two-phase flow. *Int J Multiphase Flow* 12:745
- Lahey Jr RT, Drew DA (1988) The three-dimensional time and volume averaged conservation equations of two-phase flow. In: *Advances in nuclear science and technology*. Springer, US, pp 1–69
- Lahey RT Jr, Drew DA (2001) The analysis of two-phase flow and heat transfer using a multidimensional, four field, two-fluid Model. *Nucl Eng Des* 204(1):29–44
- Lakehal D, Meier M, Fulgosi M (2002) Interface tracking towards the direct simulation of heat and mass transfer in multiphase flows. *Int J Heat Fluid Flow* 23(3):242–257
- Lakehal D, Fulgosi M, Yadigaroglu G, Banerjee S (2003) Direct numerical simulation of heat transfer at different Prandtl numbers in counter-current gas-liquid flows. *ASME J Heat Transf* 125(6):1129–1140
- Ling Y, Zaleski S, Scardovelli R (2015) Multiscale simulation of atomization with small droplets represented by a Lagrangian point-particle model. *Int J Multiphase Flow* 76:122–143
- Long LN, Micci MM, Wong BC (1996) Molecular dynamics simulations of droplet evaporation. *Comp Phys Commun* 96(2):167–172

- Meyer JE (1960) Conservation laws in one-dimensional hydrodynamics. Bettis Technical Review, p 61 <https://www.osti.gov/scitech/servlets/purl/4127649#page=68>
- Ng TS (2002) Interfacial structure in stratified pipe flow. Ph.D. thesis, University of London, June 2002
- Nigmatulin RI (1979) Spatial averaging in the mechanics of heterogeneous and dispersed systems. *Int J Multiph Flow* 5(5):353–385
- Osher S, Sethian JA (1988) Fronts propagating with curvature-dependent speed: algorithms based on Hamilton-Jacobi formulations. *J Comput Phys* 79:12–49
- Rider WJ, Kothe DB (1998) Reconstructing volume tracking. *J Comput Phys* 141:112–152
- Scardovelli R, Zaleski S (1999) Direct numerical simulation of free-surface and interfacial flow. *Annu Rev Fluid Mech* 31(1):567–603
- Shaha J (1999) Phase interactions in transient stratified flow. Ph.D. thesis, University of London, August 1999
- Spedding PL, Hand NP (1997) Prediction in stratified gas-liquid co-current flow in horizontal pipelines. *Int J Heat Mass Transf* 40(8):1923–1935
- Štrubelj L, Tiselj I, Mavko B (2009) Simulations of free surface flows with implementation of surface tension and interface sharpening in the two-fluid model. *Int J Heat Fluid Flow* 30(4):741–750
- Srichai S (1994) High pressure separated two-phase flow. Doctoral dissertation, Imperial College, London
- Sussman M, Smereka P, Osher S (1994) A level set approach for computing solutions to incompressible two-phase flow. *J Comput Phys* 114:146–159
- Taitel Y, Dukler AE (1976) A model for predicting flow regime transitions in horizontal and near horizontal gas-liquid flow. *AIChE J* 22(1):47–55
- Tryggvason G, Bunner B, Esmaeeli A, Juric D, Al-Rawahi N, Tauber W, Han J, Nas S, Jan YJ (2001) A front tracking method for the computations of multiphase flow. *J Comput Phys* 169:708–759
- Unverdi SO, Tryggvason G (1992) A front tracking method for viscous incompressible flows. *J Comput Phys* 100:25–37
- Whalley PB, Hutchinson P, Hewitt, GF (1974). The calculation of critical heat flux in forced convective boiling. Heat transfer. In: Proceedings of the 1974 International Heat Transfer Conference, vol 4, pp 290–294
- Whalley PB, Hutchinson P, James PW (1978). The calculation of critical heat flux in complex situations using an annular flow model. In: Proceedings of 6th International Heat Transfer Conference, Toronto, vol 5, pp 65–70
- Yadigaroglu G (2003) Letter to the Editor, CMFD (a brand name) and other acronyms. *Int J Multiphase Flow* 29:719–720
- Yadigaroglu G (2005) Computational fluid dynamics for nuclear applications: from CFD to multi-scale CMFD. *Nucl Eng Des* 235(2):153–164
- Yadigaroglu G, Lakehal D (2003) New challenges in computational thermal hydraulics, invited plenary lecture. In: The 10th international topical meeting on nuclear reactor thermal hydraulics (NURETH-10), Seoul, Korea, 5–9 October 2003
- Yadigaroglu G, Lahey RTL Jr (1976) On the various forms of the conservation equations in two-phase flow. *Int J Multiphase Flow* 2:477–494
- Yi P, Poulikakos D, Walther J, Yadigaroglu G (2002) Molecular dynamics simulation of vaporization of an ultra-thin liquid argon layer on a surface. *Int J Heat Mass Transf* 45: 2087–2100
- Zuber N (1967) Conservation laws for two-phase flow with a change of phase. *Int J Heat Mass Transf* 10:1637–1642
- Zuber N, Findlay (1965) Average volumetric concentration in two-phase flow systems. *J Heat Transf* 87:453–468

Introduction to Multiphase Flow

Basic Concepts, Applications and Modelling

Yadigaroglu, G.; Hewitt, G.F. (Eds.)

2018, IX, 214 p. 84 illus., 57 illus. in color., Hardcover

ISBN: 978-3-319-58717-2